



RESEARCH ARTICLE

An Automated Tool for Extraction of Crop Condition from Temporal Synthetic Aperture Radar (SAR) Data

Ragunath KP *, Pazhanivelan S and Kumaraperumal R

*Department of Remote Sensing and GIS, Tamil Nadu Agricultural University, Coimbatore-3

ABSTRACT

Crop identification and acreage estimation were challenging for remote sensing scientists, especially when cropping season coincides with monsoon due to cloud coverage in optical data. Synthetic Aperture Radar (SAR) data has proved to be an alternative for overcoming the issue of clouds during the crop growth period and aid in crop identification. Crop identification has already reached the stage of operational services using the SAR data, while the crop condition assessment is still developing due to variations in crop scattering mechanisms. Automated algorithms are promising tools for capturing the wide variation in spatial and temporal data scattering properties. The importance of automation in GIS is evident in recent years from global research. Tracking of growth stages of a crop has quantum applications in yield forecast and formulating marketing strategies. To quantify the crop condition during the crop growth period, an automated tool to capture various stages of the crop, its conditions, and documentation was developed using the preprocessed SAR images derived from a fully automated processing chain module available with MAPscape software. The outputs of temporal Band Sequential (BSQ) images and Start of Season (SOS) for the analysis crop from MAPscape software were used as input for the automation tool to extract crop conditions viz., failed sowing, crop failure, and a good crop. The backscatter signatures developed from ground truth data for various crop conditions were used to validate the product.

Received: 17 July 2022

Revised: 24 August 2022

Accepted: 27 September 2022

Keywords: SAR data;Crop condition;NDVI profile;Automated tool

INTRODUCTION

Crop identification, yield estimation, varietal discrimination, and crop condition assessment are challenges before remote sensing scientists. Many developments in crop identification and yield estimation exist, while there are few breakthroughs in assessing the crop condition temporally. The restricted or rare availability of temporal cloud-free optical data during major cropping seasons has complicated tracking the crop condition. Microwave data is the only alternate option for assessing crop conditions in areas without cloud-free optical data. In Tamil Nadu, Rabi is the major rice-growing season devoid of cloud-free optical data.

As a new technology with the advantage of all-weather, all-time, high resolution, and wide coverage, synthetic aperture radar (SAR) has been widely applied in the agricultural condition monitoring field. It thus provides a robust complement and support for crop identification. The updating and improvement of function parameters and performance index of radar

sensors have been an essential field of agriculture remote sensing that gets the information of crop acreage, growing conditions and yield by SAR. The handling of microwave data is advantageous in tropical regions in Asia, where most crops are grown in the rainy season. The processing of microwave data defies before the scientists have been overcome by software with automated processing chain. Hence, with these developments, it is now possible to take up crop condition assessment from SAR data.

Monitoring vegetation properties has received much attention among several remote sensing applications. Doriaswamy *et al.* 2004, extensively carried out the crop condition assessment and yield simulations using Landsat and MODIS. Many experimental activities (Boerner *et al.*, 1987, Haldar *et al.*, 2012) were carried out to investigate the sensitivity of microwave sensors to vegetation parameters were carried out. The use of SAR backscatter coefficient in different polarizations and frequencies for crop identification and monitoring has been reported (Toan *et al.*, 1989 & 1997;

Hoekman and Bouman, 1993; Kurosu *et al.*, 1995; Schotten *et al.*, 1995). Using a polarimetric scattering matrix that contains information about polarization amplitude as well as a phase for crop characterization and classification has also been studied (Freeman *et al.*, 1994; Skriver *et al.*, 1999; Lee *et al.*, 2001; Ainsworth *et al.*, 2009; Haldar *et al.*, 2012; Turkar *et al.*, 2012, Panigrahy *et al.*, 2013). An attempt has also been made to establish relationships between polarization signatures of SAR signal to target properties (Ulaby *et al.*, 1987; Boerner *et al.*, 1987; Wang and Mo, 1990).

SAR images for the rice area assessment have already reached the operational stage in Asian countries owing to their characteristic temporal signature. However, applying SAR images to estimate crop condition assessment is challenging, especially for understanding crop scattering mechanisms and discrimination. Automated algorithms are essential for mapping at large geographic scales (Bolanos *et al.*, 2016; Westerhoff *et al.*, 2013; Santoro *et al.*, 2015). Traditionally, selecting a training dataset is one of the tedious and subjective steps that impede the automation in either thresholding or classification algorithms. Recently, several studies demonstrated the feasibility of automatically selecting training datasets from existing data products to generate newer and enhanced products (Feng *et al.*, 2015; Klein *et al.*, 2015; Zhang *et al.*, 2017).

The importance of automation in GIS has been well understood in recent years due to its spatial and temporal variability. Information on crop conditions has the advantage of spatially assessing the yield forecast and formulating marketing strategies. Accurately quantifying the spatial and temporal dynamics of crop conditions in fields is critical. Since crop condition varies for each pixel, data consolidation is a tedious process, which warrants an automated crop condition assessment and reporting tool.

MATERIAL AND METHODS

The detection and delineation of rice crops for crop condition assessment were carried out in the Thiruvavur district of Tamil Nadu. The district is an agricultural district with rice as the main crop covering more than 90 per cent of the cultivable area. The district has a net cultivated area of around 3.28 lakh ha.

Rice area detection and delineation

Sentinel 1A SAR data, downloaded from the USGS website for 2019 at 12 days intervals. The dual-polarized Sentinel 1A data was subjected to preprocessing for further analysis of crop condition assessment following a fully automated processing chain designed by Holecz *et al.* (2013) to

convert the multi-temporal SAR data into terrain geocoded σ° values.

The defects in the raw SAR images were caused due to atmospheric interference, radiometric characteristics were initially corrected, and the temporal stacks were registered (geometrical rectification) for extracting temporal signatures of rice crop. The steps in preprocessing include Mosaicking, Co-registration, Speckle filtering, terrain geocoding, Radiometric calibration and Normalization, Anisotropic non-linear diffusion (ANLD) filtering, Removal of atmospheric attenuation, Sub-setting and Single Look Complex (SLC) processing. The processing chain is available as a module within the MAPscape software (Figure 1).

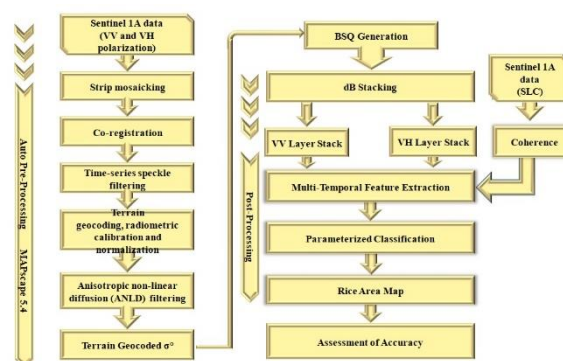


Figure 1. Multi-Temporal σ° Rule-Based Rice Detection

The multi-temporal stack of terrain-geocoded σ° images was used as input to a rule-based rice detection algorithm in MAPscape software. The temporal evolution of σ° was analyzed from an agronomic perspective, which requires a prior knowledge of rice maturity, calendar, duration and crop practices from field information and understanding of the study location. The temporal signature is frequency and polarization-dependent and depends on the crop establishment method and, to some extent, crop maturity. This implies that general rules can be applied to detect rice but that the parameters for these rules may be adapted according to the agro-ecological zone, crop practices and rice calendar.

A simple statistical analysis of the temporal signature of σ° values in the monitored fields guided the choices of parameters. The mean, minimum, maximum, minimum ratio, maximum ratio and span ratio of σ° were computed for the temporal signature of each monitored field. These six statistics, called temporal features, concisely characterize the key information in the rice signatures of the observed fields, and each relates directly to one parameter. Hence, the values of the six temporal features from the monitoring locations were used to guide the classification.

The outputs viz., BSQ images (Band Sequential), and SOS generated from the processing of temporal Sentinel 1A SAR data were used as inputs for the automation tool to derive crop conditions.

II. Ground truth and signature analysis

Tracking crop growth stages and analyzing backscattering interaction with the crop is essential to capture the crop condition. Around 200 ground-truth locations were selected across the district covering various crop growth conditions to derive temporal signatures for a detailed analysis of the signatures to understand the interaction and classify the crop condition into different classes viz., failed sowing, total crop failure and a good crop. Failed sowing is defined as a condition when the crop fails within 40 days after sowing/transplanting in the field, while total crop failure is when the crop fails after 40 days and before reaching the peak vegetative stage (< 70-80 days). The other crops were classified as good crops. Around 40 per cent of the ground truth data was used for the correlation and methodology development, and the remaining will be used to validate the tool.

III. py coding and tool (GUI) development

Python language has a separate module (pyro SAR) for programming SAR data, which can perform SAR image analysis. The correlation methodology to assess crop condition from backscatter values was incorporated into python programming to derive the desired output. A Graphical User Input (GUI) tool was developed with options to get data viz., BSQ and Start of Season images with administrative boundary. The crop condition module was designed to takes Inputs viz., BSQ file, Start of Season (SOS) file, shapefile for boundary and output folder to save the output.

Apart from the main module of crop condition, an additional module NDVI profile tool was developed to aid in further information on the historical crop condition for the test crop. The NDVI profile module takes Inputs viz., Input folder, which has the NDVI files, Shapefile for boundary and output folder to save the output. Using these as inputs, the tool performs the following steps in an automated manner.

IV. Zonation, report generation, and validation

Based on the administrative boundary input for the tool, the zonation and output report generation were automated and incorporated into the tool. Percent area distribution of various crop conditions assessed for the area will be reported as a graph and excels outputs for further analysis and interpretation. The ground truth data, which was not used for methodology development, were

used to validate the output from the tool developed. Accuracy assessments were carried out with a confusion matrix and kappa index.

V. Accuracy Assessment

The Error matrix and Kappa statistics are used for evaluating the accuracy of the estimated rice area. The class allocation of each pixel in the classified image is compared with the corresponding class allocation on reference data (Crop Cutting Experiment data) to determine the classification accuracy. The pixels of agreement and disagreement are compiled as an error matrix. The rows and columns represent the number of all classes, and the matrix elements represent the number of pixels in the testing dataset (Lillesand, 1994). The accuracy measures, such as overall accuracy, producer's accuracy, and user's accuracy, are estimated from the error matrix (Congalton, 1991). The accuracy is calculated as;

$$\text{Overall Accuracy} = \frac{\Sigma(\text{Correctly classified classes along diagonal})}{\Sigma(\text{Row Total or Column Total})} \quad (1)$$

$$\text{Producer's Accuracy} = \frac{\text{Number of correctly classified class in a column}}{\text{Total number of items verified in that column}} \quad (2)$$

$$\text{User's Accuracy} = \frac{\text{Number of correctly classified item in a row}}{\text{Total number of items verified in that row}} \quad (3)$$

Another measure of classification accuracy is the kappa coefficient, which measures the proportional (or percentage) improvement by the classifier over a random assignment to classes (Richards, 1999). The kappa coefficient is estimated from the formula for an error matrix with r rows and the same number of columns.

$$\hat{K} = \frac{NA-B}{N^2-B} \quad (4)$$

Where,

A -the sum of r diagonal elements, which is the numerator in the computation of overall accuracy

B -the sum of the r products (row total x column total)

N -the number of pixels in the error matrix (the sum of all r individual cell values)

Results and Discussion

Rice crops and their crop growth in tropical and subtropical regions can be detected and tracked precisely through Synthetic Aperture Radar (SAR) imagery, especially where cloud cover restricts optical imagery. Parameterized classification with multi-temporal features derived from regularly acquired C-band, V.V. and V.H. polarized Sentinel-1A SAR imagery

was used for mapping rice area. Nelson *et al.* (2014) demonstrated an operational-orientated effort with an extensive demonstration of rice area mapping with SAR in 13 geographical rice-growing locations across South and South-east Asia in the context of Remote Sensing-based Information and Insurance.

PMFBY crop insurance scheme implemented in India is based on the village as a unit for claiming insurance which includes various criteria, viz., prevented sowing, failed sowing, total crop failure, and yield-based compensations. Prevented sowing category is implemented when the village sown area is less than 25 per cent of the normal area sown before a cutoff date as decided by the district-level monitoring committee in that village which requires precise rice area grown in the particular village. Failed sowing is defined as a condition when the crop fails within 40 days after sowing/transplanting in the field while total crop failure is when the crop fails after 40 days and before reaching peak vegetative stage (i.e., < 70-80 days). The other crops are said to be good crop.

To estimate the various categories of PMFBY crop insurance scheme, a detailed analysis of the temporal signatures for Rice crops was carried out to understand the correlation between the phenological stages of the crop and the backscatter values from temporal SAR satellite data. The results obtained are as follows.

1. Extraction of temporal signatures to assess crop condition:

Temporal signatures were extracted for the 200 ground truth points collected during the crop survey of Thiruvarur district. The start of season map generated from processing of SAR data in Mapscape software for rice crop was used to identify the start date of each rice pixel in the map and was correlated with the phenological stages of the crop thereafter. The SAR satellite data were acquired every 12 days, and the corresponding backscatter (dB) values were plotted to identify the temporal signature of the rice crop. The analysis showed that the backscattering (dB) values increased from the start of the season (SOS) as the crop grew and reached a maximum at the peak vegetative stage / Flowering stage and started decreasing there after (Figure 2) for a normal crop. The minimum dB values ranged from -19.93 to -17.09 and the maximum from -17.23 to -15.54.

The temporal signatures extracted using ground truth data showed a decline in dB values even before attaining 90 days duration in a few spots denoting the failure of the crop (did not follow a standard growth pattern). The decline in dB was at different stages of the crop from the start. These signatures were extracted to derive the rice crop's failed and crop failure condition. The various forms of failed and crop failure signatures derived are presented in Figures 3a&b.

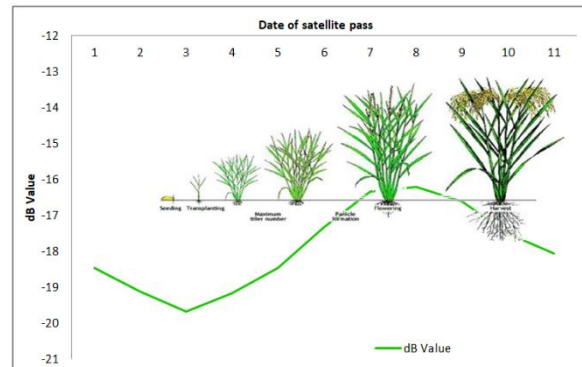
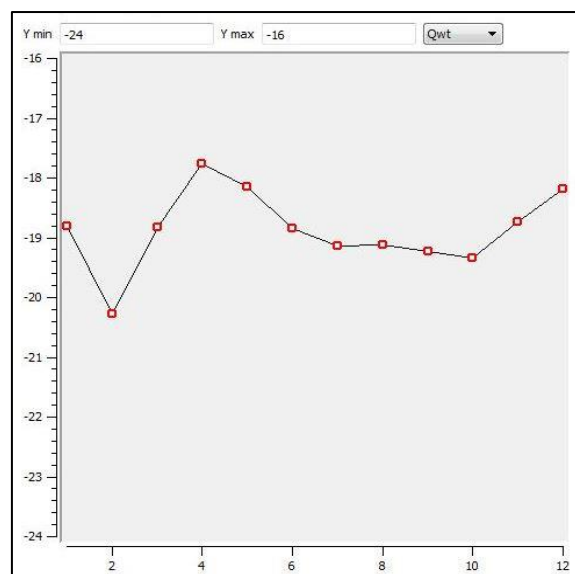
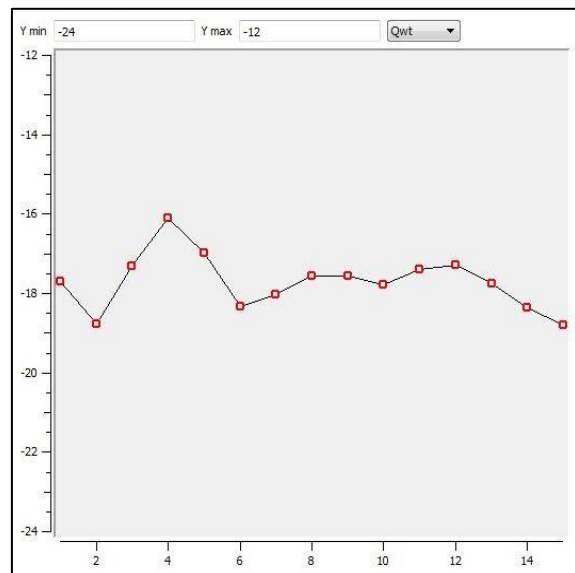


Figure 2. Mean temporal dB curve for paddy crop generated from Sentinel-1A



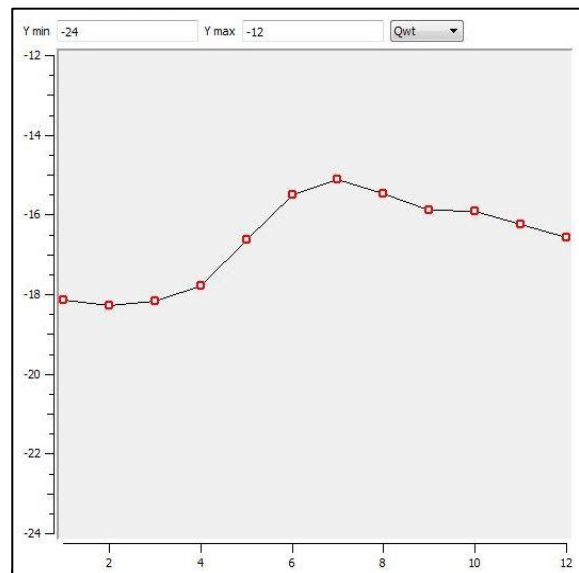
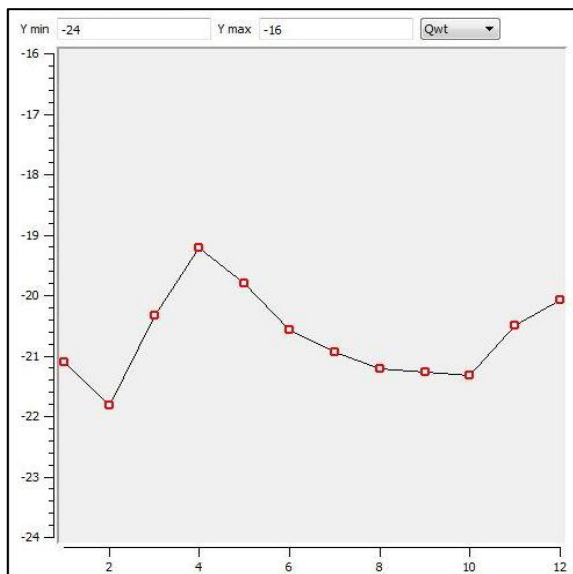
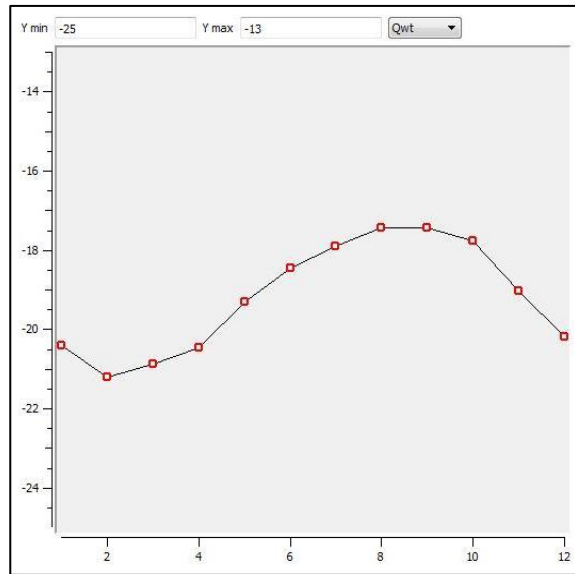
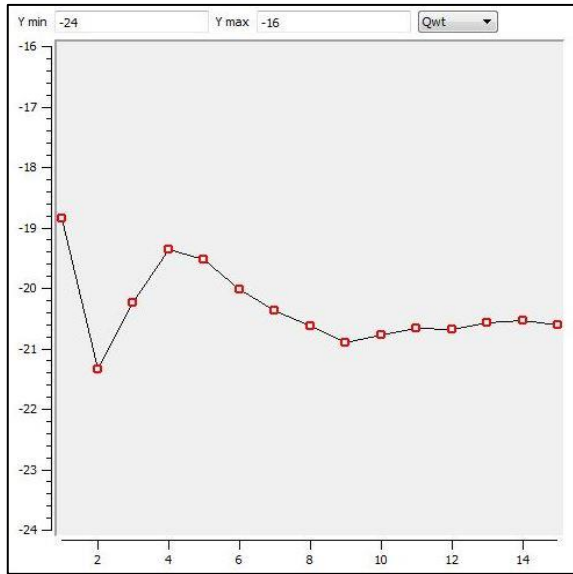


Figure 3a. Temporal Signature of Failed Sowing

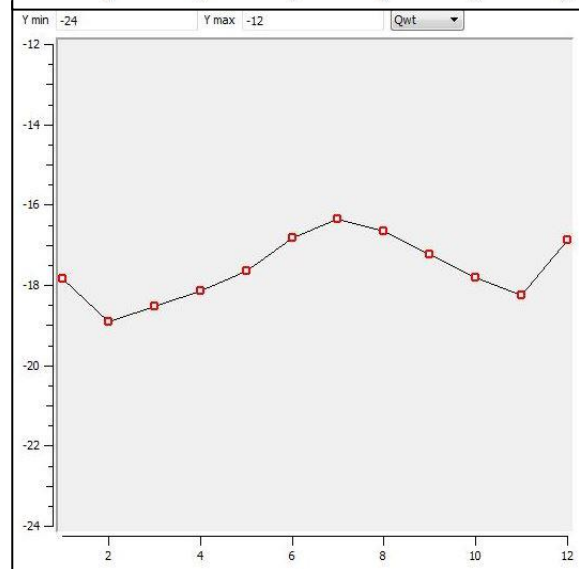
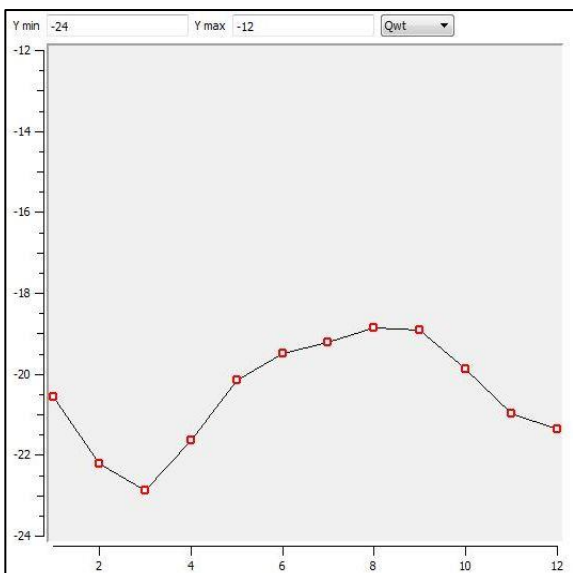


Figure 3b. Temporal Signature of Crop Failure

2. Automated processing tool for delineating various crop conditions:

Based on the knowledge acquired from the detailed analysis of crop response to temporal backscatter (dB) values, a tool to automate the extraction of temporal signature from satellite data and to classify the pixels based on the signature was developed using python script integrating Geospatial Data Abstraction Library (GDAL) and OGR libraries. Two modules viz., Crop Condition Analyst and NDVI profile analyst were developed to attain the objectives of the project. A graphical user interface (GUI) was developed to include the modules and for easy operation using Q.T.designer (Figure 4a), which consists of a main menu with drops of the two modules, Settings to provide input and output directories of work, panel hiding, etc. The Crop condition module takes Inputs viz., BSQ file, Start of Season (SOS) file, Shapefile for boundary and Output folder to save the output (Figure 4b). Using these as inputs, the tool performs the following steps in an automated manner.

- a) Extracting values from BSQ Layer: Extracting the number of bands in the BSQ layer will be done by iterating through the pixels.
- b) Preparing Mask Layer: SOS layer will be used to mask the BSQ file to keep only the rice pixels and remove no-data values and other non-rice pixels to reduce processing time.
- c) Populating classes: Each band (temporal data) will be converted to array values and iterated through the SOS pixels for deriving the temporal signature.
- d) Generating Final output class-map: The signature values extracted from the previous step will be classified as failed sowing, Crop failure, and a good crop.
- e) Zonal Statistics: Area statistics will be derived from the class image and written to excel for further processing.

The data for the Thiruvavur district of Tamil Nadu was taken up to run the tool. Block map of the district was given as boundary input, and the tool performed seamlessly, giving the image and excel outputs within 2 minutes and 45 seconds. The district had 18 blocks, and the area under each category of failed sowing, total crop failure, and good crop were delineated (Table 1).

The NDVI profile module takes inputs viz., Input folder which has the NDVI files, Shapefile for boundary, and Output folder to save the output (Figure 4c). Using these as inputs, the tool performs the following steps in an automated manner.

- a) Listing of NDVI files: The process iterates through the input folder and finds suitable images for processing. It also performs year listing from the files identified.
- b) Populating arrays: The identified NDVI files will be converted to arrays to extract values.
- c) Populating classes: Each NDVI file will be iterated through the pixels to derive the temporal signature.
- d) Generating Final output class-map: The signature values extracted from the previous step will be classified based on the number of peaks attained in a year and generate season maps.
- e) Zonal Statistics: Area statistics will be derived from the class image and written to excel for further processing.

The output generated from the modules can be visualized in the matplotlib chart output for information. Further mapping can be taken up using open-source GIS software's viz., QGIS, GRASS or SAGA. The outputs are presented in Figure 4d.

3. Accuracy assessment:

The output generated from the tool viz., Failed sowing, total crop failure and a good crop were assessed for accuracy using a confusion matrix. The Crop Cutting Experiment data collected for the study area were used for the assessment. Around 230 CCE points were collected including 136 data for good crop category and 94 points for Total crop failure. Since the study area (Thiruvavur district) did not contain failed sowing CCE points, the class was omitted for accuracy assessment. The results revealed an overall accuracy of 93.04 per cent and a kappa index of 0.85 (Table 2). The estimates of area under different categories from the tool were of good accuracy, evident from the accuracy and more than 85 percent agreement apparent from the kappa index. The tool has classified the categories with higher accuracy.

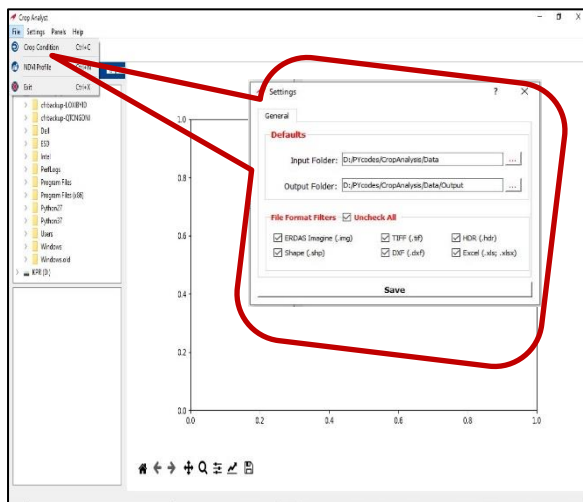


Figure 4a. Crop condition assessment tool

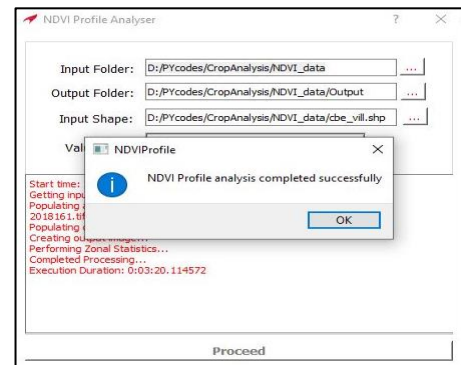


Figure 4c. NDVI Profile Analysis module

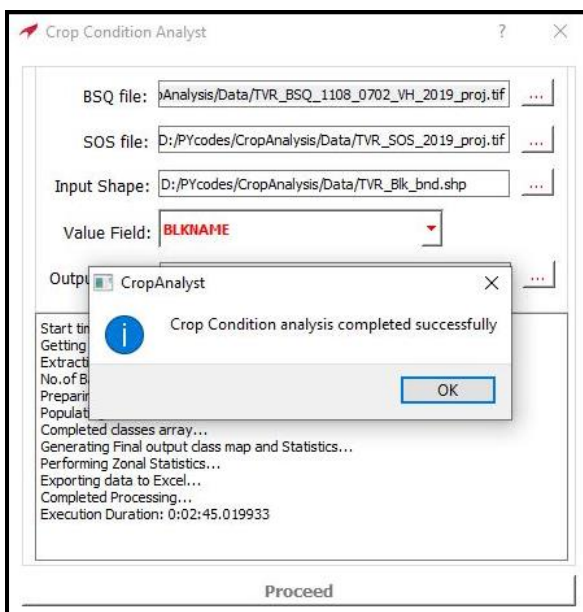
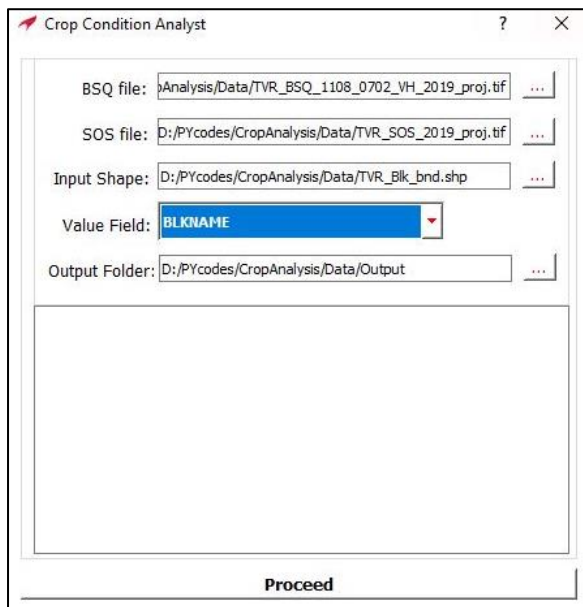


Figure 4b. Crop condition Analysis module

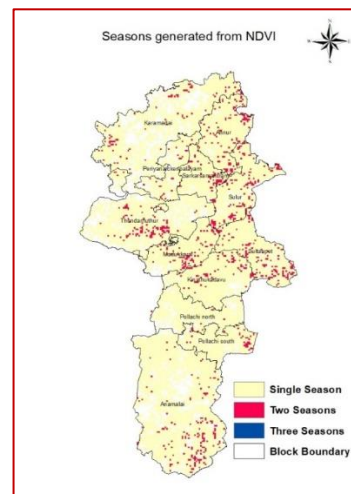
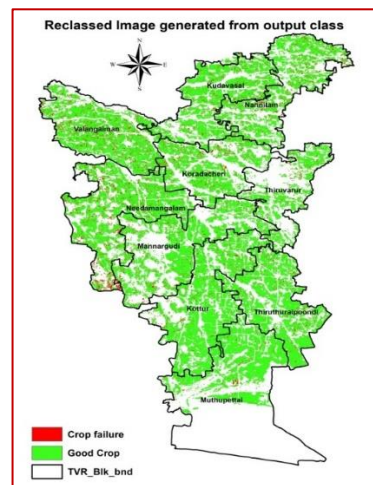


Figure 4d. Output maps generated from Crop condition tool



Table 1. Classes of Rice area in Thiruvarur district (Area in ha)

BLKNAME	Block Area	Failed Sowing	Crop Failure	Good Crop	Percent area cultivated
Thiruppanandal	16496.44	0	966.16	9501.51	63.45
Kumbakonam	18237.74	0	1342.99	10586.16	65.41
Thiruvaidaimaruthur	18858.18	0	1095.78	10032.82	59.01
Papanasam	14661.41	0	934.03	6385.17	49.92
Thiruvaiyaru	16373.19	0	1870.59	11961.23	84.48
Ammapettai	10.02	0	0.82	14.19	149.80
Ammapettai	4.61	0	1.88	2.20	88.50
Ammapettai	196.92	0	5.67	50.07	28.31
Ammapettai	123.43	0	17.25	95.08	91.01
Ammapettai	23904.89	0	2381.36	17857.24	84.66
Thanjavur	42457.59	0	4353.85	28262.00	76.82
Budalur	28730.11	0	2038.38	15518.04	61.11
Orathanadu	41134.06	0	5016.08	30350.89	85.98
Thiruvanam	21433.16	0	2163.43	14794.77	79.12
Madukkur	17665.95	0	959.23	6128.46	40.12
Pattukottai	32591.56	0	2192.58	12560.80	45.27
Peravurani	20676.45	0	1453.93	8355.90	47.44
Sethubavachatram	26507.82	0	2727.85	8267.10	41.48

Table 2. Accuracy assessment for rice classes

Actual class from CCE	Predicted class from the map			
	Class	Good Crop	Total Crop failure	Accuracy
	Good Crop	129	7	94.85%
	Total Crop failure	9	85	90.43%
	Reliability	93.48%	92.39%	93.04%
Average accuracy				92.64%
Average reliability				92.93%
Overall accuracy				93.04% (Good accuracy)
Kappa index				0.85



CONCLUSION

It is important to assess spatial and temporal crop conditions to understand the impact of waning monsoon, pest and disease incidence, and management practices, which directly affect the crop yield and, subsequently, the market. Although the estimation of crop area could be achieved with higher precision through remote sensing, obtaining information on crop conditions through the growing season is always a constraint due to high spatially and temporally variability. This issue has been overcome with the development of an in-house tool coded using Python scripting with extended GDAL and OGR libraries to process Spatio-temporal satellite data and vector files for effectively delineating crop conditions from the backscattered values. The tool can generate statistics from farm level to State or country level in a quicker time, and the outputs are presented in both image and excel formats, which can serve as a base for understanding the crop condition spatially and temporally. The automated tool developed is of open source type and is specific to rice crop condition assessment from temporal SAR satellite data, while there exists scope for extending to other crops by analyzing backscatter signatures and the crop growth cycle. Some of the hard-coded parameters for assessing the crop condition can be made as user input to make the tool more dynamic.

Funding and Acknowledgment

The authors thank the Tamil Nadu Agricultural University for providing the fund to carry out the research work in a project mode and also thank the Professor and Head and staff of the Department of Remote Sensing and GIS, TNAU for their valuable comments and constructive suggestions on the manuscript.

Ethics statement

No specific permits were required for the described field studies because no human or animal subjects were involved in this research.

Originality and plagiarism

The Authors assure that the work written and submitted is entirely original, and the work and/or words of others, that is used in the text has been appropriately cited.

Consent for publication

All the authors agreed to publish the content.

Competing interests

There were no conflict of interest in the publication of this content

Data availability

All the data of this manuscript are included in the MS. No separate external data source is required. If anything is required from the M.S., certainly, this will be extended by communicating with the corresponding author through corresponding official mail: ragunathkp@tnau.ac.in.

REFERENCES

- Ainsworth, T. L., Kelly, J. P. and Lee, J.-S., 2009. Classification comparisons between dual-pol, compact polarimetric and quad-pol SAR imagery, *ISPRS Journal of Photogrammetry and Remote Sensing*, **64**: 464-471.
- Berlin. Santoro, M.; Wegmüller, U.; Lamarche, C.; Bontemps, S.; Defourny, P.; Arino, O. 2015. Strengths and weaknesses of multi-year Envisat ASAR backscatter measurements to map permanent open water bodies at global scale. *Remote Sens. Environ.* **171**:185–201.
- Boerner, W.M., Foo, B.Y. and Eom, H.J., 1987. Interpretation of the polarimetric co-polarization phase term in radar images obtained with JPL airborne L-band SAR system, *IEEE Transactions on Geosci. and Remote Sensing*, **25(1)**: 77-82,.
- Bolanos, S.; Stiff, D.; Brisco, B.; Pietroniro, A. 2016. Operational surface water detection and monitoring using radarsat 2. *Remote Sens.*, **8**: 285.
- Congalton, Russell G. 1991. Remote sensing and geographic information system data integration: error sources. *Photogrammetric Engineering & Remote Sensing*, **57(6)**:677-687.
- Doraiswamy, P. C., J. L. Hatfield, T. J. Jackson, B. Akhmedov, J. Prueger, and A. Stern. 2004. Crop Condition and Yield Simulations Using Landsat and MODIS. *Remote Sensing of Environment* **92**: 548–59.
- Feng, M.; Sexton, J.O.; Channan, S.; Townshend, J.R. 2015. A global, high-resolution (30-m) inland water body dataset for 2000: First results of a topographic-spectral classification algorithm. *Int. J. Digit. Earth.*, 1–21
- Freeman, J., Villasenor, J. D., Klein, H. P. and Groot, J., 1994. On the use of multi-frequency and polarimetric radar backscatter features for classification of agricultural crops, *Int. J. Remote Sensing*, **15(9)**:1799-1812.
- Haldar, D., Das, A., Mohan, S., Pal, O., Hooda, R.S. and Chakraborty, M., 2012. Assessment of L-band SAR data at different polarization combinations for crop and other land use classification. *Prog. In Electromagnetic Research B. (PIER)*, **36**: 303-321.
- Hoekman, D. H. and Bouman, B. A. M., 1993. Interpretation of C- and X-band radar images over an agricultural area, the Flevoland test site in the agriscatt-87 campaign, *International Journal of Remote Sensing*, **14**:1577-1594,



- Holecz, Francesco, Massimo Barbieri, Francesco Collivignarelli, Luca Gatti, Andrew Nelson, Tri DeriSetiyono, MircoBoschetti, GiacintoManfron, Pietro Alessandro Brivio, and JE Quilang. 2013. An operational remote sensing based service for rice production estimation at national scale. Proceedings of the living planet symposium.
- Klein, I.; Dietz, A.; Gessner, U.; Dech, S.; Kuenzer, C. 2015. Results of the global waterpack: A novel product to assess inland water body dynamics on a daily basis. *Remote Sens. Lett.*, **6**:78–87.
- Kurosu, T., Fujita, M. and Chiba, K., 1995. Monitoring of rice crop growth from space using the ERS-1 C-band SAR, *IEEE. Trans. Geosci. Remote Sensing*, **33**:1092–1096,
- Lee, J.-S., M. R. Grunes, and E. Pottier, 2001. Quantitative comparison of classification capability: Fully polarimetric versus dual-and single-polarization SAR, *IEEE Transactions on Geosci. and Remote Sensing*, **39(11)**: 2343-2351,
- Lillesand, Thomas M. 1994. Strategies for improving the accuracy and specificity of large-area, satellite-based land cover inventories. *International Archives of Photogrammetry and Remote Sensing* **30**:23-30.
- Panigrahy R.K. and A K Mishra.2013. An Unsupervised Classification of scattering behaviour using Hybrid Polarimetry. *IET Radar, Sonar & Navigation*, **7(3)**:270- 276.
- Richards, J.A., Jia, X., 1999. *Remote Sensing Digital Image Analysis, an Introduction*. Third ed. Springer, ISBN: 9783030823276.
- Schotten, C. G. J., Van Rooy, W. W. L. and Janssen, L. L. F., 1995. Assessment of the capabilities of multi-temporal ERS-1 SAR data to discriminate between agricultural crops, *Int. J. Remote Sensing*, **16(14)**: 2619-2637,
- Skriver, H., Morten, T. S. and Thomsen, A. G., 1999. Multitemporal C and L-band polarimetric signatures of crops, *IEEE Transactions on Geosci. and Remote Sensing*, **37(5)**: 2413-2429,
- Toan, L. T., H. Laur, E. Mougin, and A. Lopes, 1989. Multitemporal and dual-polarization observations of agricultural vegetation covers by X-band SAR images, *IEEE Trans. Geosci. Remote Sensing*, **27**:709–717
- Toan, L.T., Ribbes, F., Wang, L. F., Floury, N., Ding, K. H., Kong, J. A., Fujita, M. and Kurosu, T., 1997. Rice crop mapping and monitoring using ERS-1 data based on experiment and modeling results, *IEEE Trans. Geosci. Remote Sensing*, **35**: 41–56,
- Turkar, V., Deo, R., Rao, Y.S., Mohan, S. and Das, 2012. A Classification accuracy of multi-frequency and multi-polarization SAR images for various land covers, *IEEE Journal of Selected Topics in Applied Earth Observations and Remote Sensing*, **5(3)**:936 – 941,
- Ulaby, F.T., Held, D., Dobson, M.C., McDonald, K.C. and Thomas, B.A., 1987. Relating polarization phase difference (PPD) of SAR signals to scene properties, *IEEE Transactions on Geosci. and Remote Sensing*, **25(1)**:.83-91,
- Wang, J.R. and Mo T., 1990. The polarization phase difference of orchard trees, *International Journal of Remote Sensing*, **11(7)**:1255-1265,.
- Westerhoff, R.; Kleuskens, M.; Winsemius, H.; Huizinga, H.; Brakenridge, G.; Bishop, C. 2013. Automated global water mapping based on wide-swath orbital synthetic-aperture radar. *Hydrol. Earth Syst. Sci.* **17**: 651–663.
- Zhang, H.K.; Roy, D.P. 2017. Using the 500 m MODIS land cover product to derive a consistent continental scale 30 m Landsat land cover classification. *Remote Sens. Environ.* **197**:15–34.